Magnetosheath Plasma Turbulence and Its Spatiotemporal Evolution as Observed by the Cluster Spacecraft

E. Yordanova
Swedish Institute of Space Physics, Uppsala, Sweden and Space Research Institute, Sofia, Bulgaria

A. Vaivads, M. André, and S. C. Buchert
Swedish Institute of Space Physics, Uppsala, Sweden

Z. Vörös
Space Research Institute, Graz, Austria and Institute of Atmospheric Physics, Prague, Czech Republic
(Received 19 June 2007; published 21 May 2008)

We study the plasma turbulence, at scales larger than the ion inertial length scale, downstream of a quasiparallel bow shock using Cluster multispacecraft measurements. We show that turbulence is intermittent and well described by the extended structure function model, which takes into account the spatial inhomogeneity of the cascade rate. For the first time we use multispacecraft observations to characterize the evolution of magnetosheath turbulence, particularly its intermittency, as a function of the distance from the bow shock. The intermittency significantly changes over the distance of the order of 100 ion inertial lengths, being increasingly stronger and anisotropic away from the bow shock.

DOI: 10.1103/PhysRevLett.100.205003 PACS numbers: 52.35.Ra, 52.35.Tc, 94.30.cj

Space is a laboratory of plasma turbulence accessible to detailed *in situ* measurements. The plasma and fluid observations suggest that turbulence is intermittent [1–4]; i.e., the spatial distribution of turbulent eddies is not uniform and becomes less space-filling towards smaller scales. The intermittency is also influenced by the presence of coherent structures (flux tubes, vortices, double layers, etc.), which existence is ignored in the classical Kolmogorov (fluid) and Kraichnan [magnetohydrodynamic (MHD)] turbulence phenomenologies. For example, in the solar wind and Earth's magnetosphere, a dominant form of the coherent structures is the Alfvenic flux tubes ([5] and references therein). The nonlinear interaction between the migrating flux tubes can result in the appearance of sheetlike filaments which may reconnect locally [6]. Recent observations reveal that reconnection downstream of Earth's bow shock (BS) occurs in many small-scale magnetic islands within thin current sheets [7], which in turn provide an effective energy dissipation mechanism [8] and could be responsible for the intermittency in the observed magnetic field fluctuations.

Using the advantages of Cluster multipoint spacecraft measurements, we investigate the development of turbulence in the magnetosheath downstream of the quasiparallel BS (the shock normal is at a small angle to the upstream magnetic field), where the solar wind plasma is slowed down and heated [9]. The magnetosheath downstream of the quasiparallel BS is one of the most turbulent plasma environments in near Earth space with the magnetic field and plasma density fluctuation amplitudes being comparable to the background level [10]. We study an event during which the Cluster spacecraft C1, C2, C3, and C4 separation is several Earth radii (Re). The separation is of the order of the turbulence integral length, and therefore it is possible to observe the development of magnetic field turbulence and its intermittency properties with the distance from the BS. The analyzed 4 min interval is the longest period of relatively stable solar wind conditions with quasiparallel geometry of the BS during which all spacecraft are in the turbulent environment of the magnetosheath. The respective time series of the magnetic field fluctuations is stationary and long enough to assure statistically confident results. We adopt the Taylor hypothesis in order to replace temporal scales with spatial ones (not shown), the validity of which could be tested with short spacecraft separation using the approach in [11].

Figure 1(a) shows magnetic field component B_Z as observed by Cluster. Upstream of the shock there are little fluctuations in B_Z while downstream of the shock in the magnetosheath fluctuations become strong with their amplitude being comparable to the background magnetic field values. The sequence in which spacecraft cross the BS is consistent with the spacecraft configuration in the model BS reference frame, Fig. 1(b). The true BS direction cannot be estimated in this case, but from previous studies it is known that there are small discrepancies between the direction predicted by model and the observed direction. C1 is the first to cross the BS around 20:49 followed by C2, C3, and C4, around 20:58. The BS is moving slightly back and forth, and around 21:13 C3 and C4 are in the BS while after that time for the rest of the interval all spacecraft are in the magnetosheath.

Figure 2 shows the power spectra of B_Z for all spacecraft. For a closer study we choose frequency interval 0.33–2.5 Hz. Taking into account the solar wind velocity in the magnetosheath, 375 km/s, the corresponding spatial

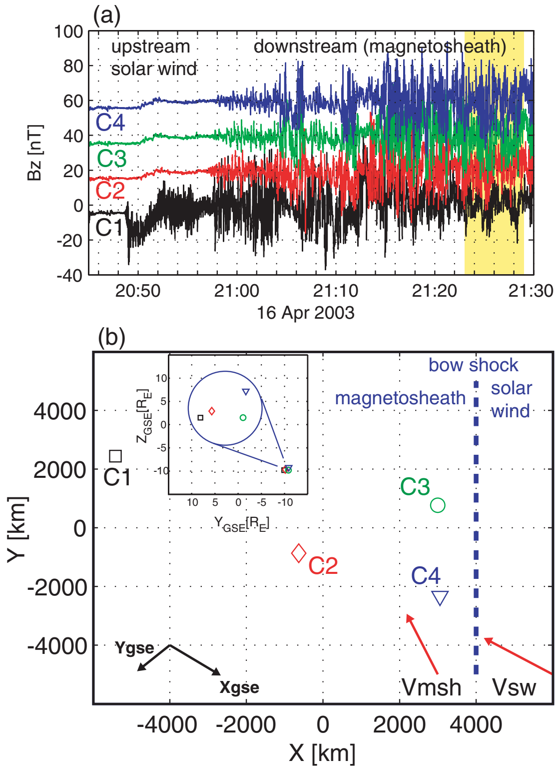

FIG. 1 (color). Overview of the event, (a) B_Z component; the different spacecraft observations are offset by 20 nT for clarity. The 4 min interval that is analyzed in details is marked in yellow. (b) Cluster configuration in the reference frame defined by the BS model, where X is along the BS normal, Y is in the plane defined by the solar wind velocity and X direction, and Z completes the frame. Also shown are the projections of the geocentric solar ecliptic system (GSE) X and Y directions. Solar wind and magnetosheath velocity directions are indicated by red arrows. The orientation of the BS is indicated by stretched line; the distance of spacecraft to the BS is discussed in text. The inset shows spacecraft location in the YZ GSE plane together with a zoom in of spacecraft configuration.

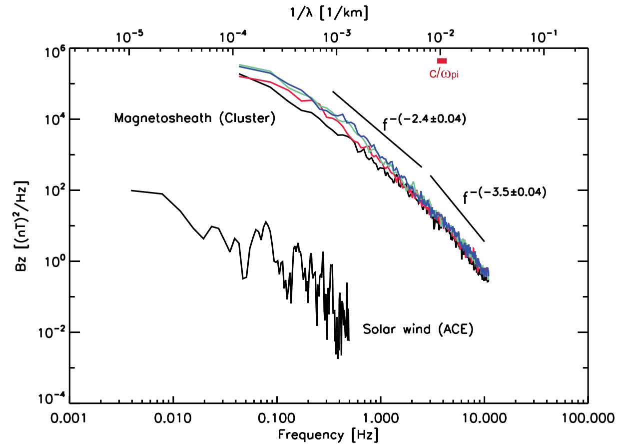

FIG. 2 (color). B_Z power spectral densities from all spacecraft for the analyzed time interval with overplot solar wind spectra for the interval 20:30–20:34 UT. Wavelengths are given at the top. The power spectral densities are characterized by two power laws—the first (marked with the shifted black line) is covering the respective frequency range, and the second one characterizes the higher frequencies (3–10 Hz). The spectrum in solar wind has different spectral slope and much smaller power spectral density.

scales are in the range 150–1100 km or $2-15c/\omega_{pi}$. Thus we investigate scales from a few to above ten ion inertial lengths. Figure 2 shows that on average C1 sees the smallest amplitude fluctuation in this frequency interval; thus, the amplitude of the fluctuations decrease with a distance from the BS (C1 is located farthest from the BS). The two power law regimes of the spectra indicate absence of long range scale invariance. It is interesting to note that the spectral index of ~ -2.5, which is known to be near the "electron MHD" or some interpretations of Hall MHD at scales smaller than c/ω_{pi} [12], and also near the average slope in the solar wind above the Hall wave number [13,14], we observe at scales larger than the ion inertial scale. Similar spectral shapes were observed also in other magnetospheric turbulent regions [15,16] and appear to be intrinsic for the near Earth plasmas. It is known from earlier studies that the self-similar ranges in the magnetosheath turbulence are much shorter than in solar wind [9], and the scaling exponents can be estimated for narrow range scales.

Commonly, the statistical properties of turbulence are studied analyzing structure functions (SF) defined from the velocity field increments across spatial scale l: $S^p(l) = \langle|v(x-l)-v(x)|^p\rangle \sim l^{\zeta_p}$. We instead study the scaling properties of the magnetosheath turbulence using the wavelet transform modulus maxima method (WTMM) [17]—an advanced method based on the continuous wavelet transform (CWT). Applying WTMM at a given scale, one calculates the partition function (PF) of a function g, as the sum over local maxima of the modulus of the wavelet transform: $Z(q,a) = \sum_{l\in L(a)}(\sup_{a'\le a}|T_g^\psi(b_l(a'),a')|)^q$, where the analyzing (mother) wavelet $T_g^\psi(b,a)$ is the 4th order Gaussian, $L(a)$ is a set of all the maxima lines l existing at a scale a, and $b_l(a)$ is the position, at a, of the maximum belonging to the line l. For self-similar time series the partition function along the lines connecting the modulus maxima scales like $Z(q,a) = a^{\tau(q)}$. The efficiency of the WTMM method over the SF approach is [18]: (1) CWT is easily adjustable to the singular signal with proper analyzing wavelet, and (2) being a sum over the modulus of the wavelet coefficients' maxima, the PF does not diverge for negative moments and covers the full set of singularities, unlike the SF that can diverge for $p<0$ because there is a nonzero probability to encounter an increment of value 0. However, for the WTMM method one should make the proper choice of analyzing wavelet, which can be uncertain and strongly dependent on the number of sampling points, the relative amplitudes of the regular and singular parts in the signal, etc. [17].

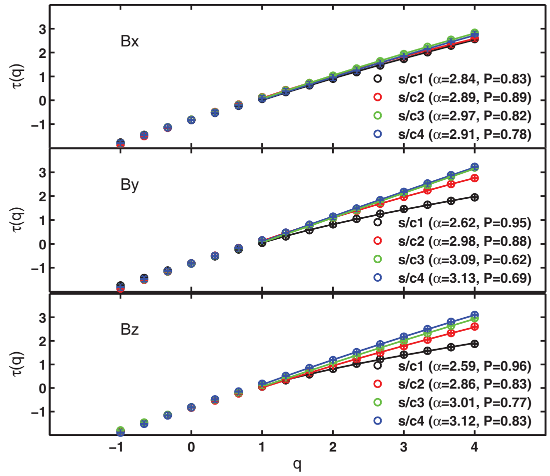

FIG. 3 (color). The scaling exponents $\tau(q)$ for B_X, B_Y, and B_Z for all Cluster spacecraft. The error bars are in the circles. The lines represent the best fit with the extended structure function model with Kolmogorov scaling.

Because of the uncertainty of higher order moments (as discussed, e.g., in [9,19]), we limit ourselves to the study of the scaling exponents in the range $q \in [-1, 4]$. Figure 3 shows the scaling exponents for all spacecraft and all magnetic field components. Experimental observations are shown by filled circles, and a few results can be clearly seen. First, the scaling exponent from different spacecraft shows almost identical behavior in B_X (the component that is normal to the BS) while scaling exponents significantly differ between spacecraft in B_Y and B_Z. Thus there is a clear anisotropy in the turbulence development in different components of the magnetic field. Second, the scaling exponents do not show linear relations indicating an intermittent character of fluctuations. This is particularly clearly seen on C1. Third, the values of the scaling exponents $\tau(q)$ for each spacecraft decrease following the order in which the spacecraft are located with respect to the BS. Thus the highest values are observed for C4 and C3, which are closest to the BS, followed by smaller $\tau(q)$ of C2 located farther in the magnetosheath, and the farthest C1 has the smallest exponents. This order is very well pronounced for the higher moments q of B_Y and B_Z. The higher nonlinearity of the $\tau(q)$ curve correspond to a stronger intermittency. A similar result of an enhanced intermittency the further one goes from the source of the turbulence was found in the heliosheath [20].

To describe quantitatively the intermittency development we fit to the data different theoretical models representing the scaling laws of the intermittent turbulence [2]. One of the models giving the best description of the intermittent fully developed solar wind turbulence [21–23] is the P model, in which the measure for the spatial inhomogeneity of the cascade rate is the P parameter [24], ($P = 0.5$ gives no intermittency, $P = 1$—fully intermittent turbulence, $P \sim 0.7$—solar wind). In the present Letter, the best fit of the experimental scaling exponents was derived for the so-called extended structure function model [25], which includes both the intrinsic spectral slope α of the energy cascade and the aforementioned intermittency parameter P. We limit the fit to the positive moment interval (1, 4) where all models can be applied. The fit of the model with different scalings (Kolmogorov for fluid, or Kraichnan for MHD turbulence) is indistinguishable. From the best fit, represented with the solid line in Fig. 3, we get α and P (the values are shown in Fig. 4). There is clear anisotropy in the behavior of both P and α as functions of the distance to the BS. Close to it, the intermittency parameter P of the magnetic field components in the shock plane (B_Y and B_Z) has smaller values than the P of B_X, which is along the shock normal. At larger distance, the intermittency in B_Y and B_Z increases and exceeds the intermittency of B_X. C1, which is the deepest in the magnetosheath, observes the most intermittent turbulence in the perpendicular to the shock plane. The spectral index α of B_X stays approximately constant with the distance from the BS, whereas α of B_Y and B_Z steadily decrease.

The same analysis was applied to the high frequency (3–10 Hz) magnetic field fluctuations. The scaling properties of the structure functions (not shown) reveal quite different behavior from that of the fluctuations in the range 0.33–2.5 Hz. There is no quantitative difference among the $\tau(q)$ values for all spacecraft and all components, indicating an isotropic turbulence at the small scales (25–125 km). The steepening of the spectra ($a \sim 2.6$–3.2) for frequencies higher than the proton gyrofrequency can be attributed to dispersive nonlinear processes due to the ion and electron motion decoupling (Hall effect); however, this effect has no influence in the case of inhomogeneous turbulence [26]. The scaling index can also change due to larger anomalous viscosity with respect to resistivity. Below the viscous cutoff, where the anomalous resistivity is negligible, the magnetic structures can evolve to smaller scales [27].

Theoretically the anisotropy in the structure function is related to the presence of a strong background magnetic

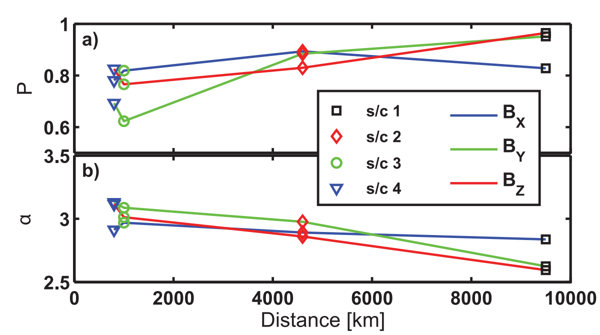

FIG. 4 (color). Intermittency parameter P (panel a) and spectral slope α (panel b) as functions of the BS distance. The colors represent the magnetic field components—B_X (blue), B_Y (green), and B_Z (red), with the spacecraft symbol in color for each P estimation.

field [28]. It increases the intermittency in the plane perpendicular to the main field and results in flattening of the spectrum of the transverse modes. In our case, the amplitude of the fluctuations is much bigger than the background field, with a slight prevalence of stronger magnetic field along B_X component. A possible interpretation of our observations could be that the larger scale background magnetic field defines the average direction of the flux tube elongation, with an additional local field vector randomly wandering about the main direction. Thus, each spacecraft may cross different flux tubes, bent because of the strongly fluctuating local magnetic field, which results in the enhanced intermittency [29]. On the other hand, the scaling exponents obtained in simulation runs with different ratios of the mean fields and fluctuations show that the intermittency (the nonlinearity of the scaling exponents curves) is higher for stronger background fields [28]. This we also observe—the most distant from the BS spacecraft 1, for which P has the highest values (see Fig. 4), has measured the strongest mean field with weakest fluctuations.

Anisotropic spectra have been also observed by Cluster close to the magnetopause, where it was suggested that the dominated by mirror modes turbulence is controlled by the background magnetic field and the magnetopause normal [30]. Similarly, the Cluster fleet is located close to the BS in our case, and as we have shown the magnetosheath turbulence properties are modified with respect to the BS normal.

In this Letter, we demonstrated for the first time that simultaneous multipoint Cluster measurements provide the ability to reveal the spatiotemporal development of intermittent and anisotropic turbulence in the magnetosheath just behind Earth's bow shock.

E. Y. would like to thank A. W. Wernik and M. Grzesiak for the WTMM algorithm, and A. Noullez and V. Carbone for the fruitful discussions. We also thank the ACE MAG and SWEPAM instruments teams, and the ACE Science Center for providing the ACE data.

[1] U. Frisch, *Turbulence: The Legacy of A. N. Kolmogorov* (Cambridge University Press, Cambridge, England, 1995).
[2] V. Carbone, P. Veltri, and R. Bruno, Nonlin. Proc. Geophys. **3**, 247 (1996).
[3] E. Marsch and C.-Y. Tu, Nonlin. Proc. Geophys. **4**, 101 (1997).
[4] L. F. Burlaga, J. Geophys. Res. **98**, 17 467 (1993).
[5] T. Chang, S. W. Y. Tarn, and C.-C. Wu, Space Sci. Rev. **122**, 281 (2006).
[6] W. H. Matthaeus and S. L. Lamkin, Phys. Fluids **29**, 2513 (1986).
[7] A. Retino, D. Sundkvist, A. Vaivads, F. Mozer, M. Andre, and C. J. Owen, Nature Phys. **3**, 236 (2007).
[8] D. Sundkvist, A. Retino, A. Vaivads, and S. D. Bale, Phys. Rev. Lett. **99**, 025004 (2007).
[9] T. Dudok de Wit and V. V. Krasnosel'skikh, Nonlin. Proc. Geophys. **3**, 262 (1996).
[10] N. Omidi, X. Blanco-Cano, and C. T. Russell, J. Geophys. Res., [Space Phys.] **110**, A12212 (2005).
[11] Z. Voros, M. P. Leubner, and W. Baumjohann, J. Geophys. Res., [Space Phys.] **111**, A02102 (2006).
[12] D. Biskamp, *Magnetohydrodynamic Turbulence* (Cambridge University Press, Cambridge, England, 2003).
[13] R. J. Leamon, C. W. Smith, N. F. Ness, W. H. Matthaeus, and H. K. Wong, J. Geophys. Res. **103**, 4775 (1998).
[14] C. W. Smith, B. J. Vasquez, and K. Hamilton, J. Geophys. Res. **111**, A09111 (2006).
[15] L. Zelenyi and A. V. Milovanov, Phys. Usp. **47**, 749 (2004).
[16] E. Yordanova, J. Bergman, G. Consolini, M. Kretzschmar, M. Materassi, B. Popielawska, M. Roca-Sogorb, K. Stasiewicz, and A. W. Wernik, Nonlin. Proc. Geophys. **12**, 817 (2005).
[17] J. F. Muzy, E. Bacry, and A. Arneodo, Phys. Rev. E **47**, 875 (1993).
[18] J. F. Muzy, E. Bacry, and A. Arneodo, Int. J. Bifurcation Chaos Appl. Sci. Eng. **4**, 245 (1994).
[19] Z. Voros, W. Baumjohann, R. Nakamura, A. Runov, M. Volwerk, T. L. Zhang, and A. Balogh, Phys. Plasmas **11**, 1333 (2004).
[20] L. F. Burlaga, N. F. Ness, and M. H. Acuna, J. Geophys. Res., [Space Phys.] **111**, A09112 (2006).
[21] C. Pagel and A. Balogh, Nonlin. Proc. Geophys. **8**, 313 (2001).
[22] V. Carbone, Ann. Geophys. **12**, 585 (1994).
[23] T. S. Horbury and A. Balogh, Nonlin. Proc. Geophys. **4**, 185 (1997).
[24] C. Meneveau and K. R. Sreenivasan, Phys. Rev. Lett. **59**, 1424 (1987).
[25] A.-Y. Tu, E. Marsch, and H. Rosenbauer, Ann. Geophys. **14**, 270 (1996).
[26] W. H. Matthaeus, P. Dmitruk, D. Smith, S. Ghosh, and S. Oughton, Geophys. Res. Lett. **30** 2104 (2003).
[27] J. Cho, A. Lazarian, and E. T. Vishniac, Lect. Notes Phys. **614**, 56 (2003).
[28] J. V. Shebalin, W. H. Matthaeus, and D. Montgomery, J. Plasma Phys. **29**, 525 (1983).
[29] R. Bruno, V. Carbone, P. Veltri, E. Pietropaolo, and B. Bavassano, Planet. Space Sci. **49**, 1201 (2001).
[30] F. Sahraoui, G. Belmont, L. Rezeau, N. Cornilleau-Wehrlin, J. L. Pingon, and A. Balogh, Phys. Rev. Lett. **96**, 075002 (2006).